A Calbindin D_{9k} Mutant with Reduced Calcium Affinity and Enhanced Cooperativity. Metal Ion Binding, Stability, and Structural Studies†

Sara Linse,* Niels R. Bylsma, Torbjörn Drakenberg, Peter Sellers, Sture Forsén, and Eva Thulin

Physical Chemistry 2, Lund University, Chemical Centre, P.O. Box 124, S-221 00 Lund, Sweden

L. Anders Svensson, Irina Zajtzeva,‡ Vjacheslav Zajtsev,‡ and Jaromir Marek§

Molecular Biophysics, Lund University, Chemical Centre, P.O. Box 124, S-221 00 Lund, Sweden

Received June 29, 1994; Revised Manuscript Received August 3, 1994®

ABSTRACT: In the native calcium-binding protein calbindin D_{9k} (M_r 8.700; 75aa; 2 EF-hands), the backbone carbonyl oxygen of Glu60 coordinates the Ca^{2+} ion in the C-terminal site (site II). The carboxylate group of the same residue forms a hydrogen bond to a water molecule that constitutes a Ca^{2+} ligand in the N-terminal site (site I). The mutant E60D, with the charge-conserving substitution Glu60→Asp, has been prepared to study the role of Glu60 in subjoining the two Ca^{2+}-binding sites and its role in the cooperative Ca^{2+} binding. Ca^{2+}-binding studies of the mutant show that the overall affinity for calcium has decreased by a factor of 38 in comparison with wild-type calbindin D_{9k}. The largest reduction is seen in the first macroscopic binding step. The Ca^{2+} affinities for both sites in the protein are reduced to a similar extent. In contrast, the mutation leads to a large increase in the cooperativity of calcium binding. Differential scanning calorimetry has been used to determine the thermal stability which is almost as high as in the wild-type protein. Cadmium binding has been assessed with ^1H and ^{113}Cd NMR. X-ray crystallographic studies of the E60D mutant in its calcium-bound form show very small structural changes relative to the wild-type protein. Almost all differences are within the error limits of the method. The largest crystallographic effects are seen in the crystal packing. Two E60D molecules with slightly different structure are found in the asymmetric unit in contrast to the single molecule in the wild-type crystal. The distance between the carboxylate group of residue 60 and the Ca^{2+}-coordinating water in site I has increased by 0.2–0.3 Å. The distance between the side chain oxygen of Gln22 and the Ca^{2+} coordinating water in site II has increased by 0.7 Å in one of the E60D molecules but is unchanged in the other. Shortening of the side chain in position 60 is therefore suggested to lead to more labile water ligands, which in part could explain the lower calcium affinity. ^1H NMR chemical shift analyses in the apo and calcium-loaded forms show that also in solution the structural consequences of the mutation are minor. The NMR results for the calcium form are in perfect agreement with the crystallographic structure determination; all chemical shift changes beyond the error limits occur for residues for which a small but significant rearrangement is observed in the crystal.

Several proteins in the calmodulin superfamily bind calcium ions with high affinity and positive cooperativity. The calcium-binding entities in these proteins are helix–loop–helix motifs known as EF-hands. There is now a wealth of experimental data on the binding constants of wild-type as well as mutant forms of many EF-hand proteins. The absolute affinity in a particular case is the net result of a large number of contributing factors (McPhalen et al., 1991; Linse & Forsén, 1995). There appears to be no straightforward formula for calculating the calcium affinity for an EF-hand of a given amino acid sequence. One of the main reasons for the lack of such a simple rule is that EF-hands normally occur in pairs, and the influence of the partner EF-hand is considerable. Isolated peptide fragments comprising single EF-hands form homodimers, but the calcium affinity for an EF-hand in such a homodimer is often several orders of magnitude lower than for the same EF-hand in its natural context, i.e., paired with an EF-hand of different sequence (Finn et al., 1992; Shaw et al., 1991; Linse et al., 1993; Reid, 1990; Kay, 1991; Tsuji, 1991). The affinity of a particular EF-hand can also be altered by making a chimera, i.e., pairing it with an EF-hand from another protein (George et al., 1993). Mutational studies have shown that amino acid substitutions within one EF-hand in a protein can have strong effects on the affinity for the partner EF-hand (Linse et al., 1988, 1991; Maune et al., 1992; Trigo-Gonzales et al., 1993).

An important property of an EF-hand pair is the cooperativity of calcium binding, or its energetic equivalent, $\Delta\Delta G$, the free energy coupling between the calcium-binding events at the two sites. Quantitative predictions of this parameter are difficult because the molecular mechanism of the cooperativity is not fully understood. The assessment of such a mechanism is the main goal of a large number of experimental studies. For example, extensive high-resolution NMR studies have aimed at a detailed description of the structure and dynamics of half-saturated states with a metal ion in one of the sites only (Akke et al., 1991, 1993; Skelton et al., 1992; Carlström et al., 1993; B. Wimberley and W. J. Chazin, personal communication). The results of these studies have led to the suggestions that, although the cooperativity in energetic terms is a property of symmetry, in molecular terms it is transmitted differently in the two calcium-binding pathways. Available data on mutant proteins show that charged residues in the loop regions are of importance for the

† This present work was supported by grants from the Swedish National Science Research Council (K-KU 10178-302 and K-KU 02545-319).

* Address correspondence to this author.

‡ Present address: SERC Daresbury Laboratory, Daresbury, Warrington, Cheshire WA44AD, U.K.

§ Present address: Department of Inorganic Chemistry, Masaryk University, Kotlářská 2, 611 37 Brno, Czech Republic.

® Abstract published in *Advance ACS Abstracts,* September 1, 1994.

0006-2960/94/0433-12478$04.50/0

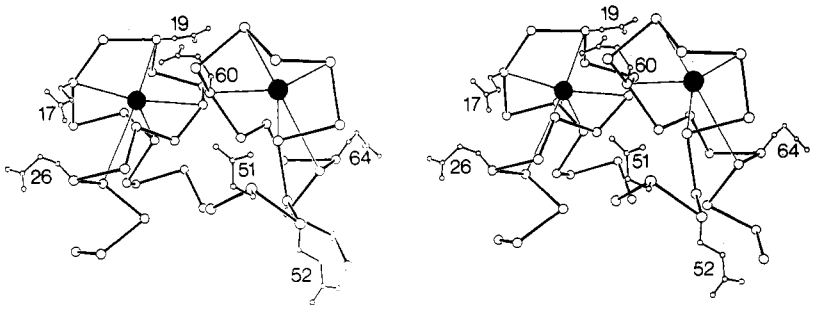

FIGURE 1: Stereview of the region around the two Ca^{2+}-binding sites of calbindin D_{9k}. The coordinates are from the crystal structure as determined by Szebenyi et al. (1986).

cooperativity in EF-hand pairs of calbindin D_{9k} and calmodulin (Linse et al., 1991; Waltersson et al., 1993). In the case of calbindin D_{9k}, there is a substantial reduction of $-\Delta\Delta G$ upon salt addition, which confirms that electrostatic interactions are important in the mechanism behind the cooperativity (Linse et al., 1991; Kesvatera et al., 1994).

The present study concerns a charge conservation mutation in calbindin D_{9k}, a protein with a single EF-hand pair. The structure of the fully calcium-loaded form of this protein has been solved to high resolution with both X-ray crystallography (Szebenyi & Moffat, 1986; Svensson et al., 1992) and NMR (Kördel et al., 1993). The structures obtained with these two methods are virtually identical. However, in the calcium-binding loops there is a scarcity of NMR-derived structural constraints leading to a much lower structural definition in solution than in the crystal. The structure of the calcium-free protein has been solved using multidimensional NMR (Skelton et al., 1994), but attempts to crystallize this form have as yet been unsuccessful. The structures reveal that charge distribution of calbindin D_{9k} is asymmetric with a predominance of negative charges in and around the calcium sites. In a previous study (Linse et al., 1991), we investigated the role of four negative charges that are present on the surface of calbindin D_{9k} in the vicinity of the calcium sites but not directly coordinating the bound Ca^{2+} ions—the side chains of Glu17, Asp19, Glu26, and Glu60 (cf. Figure 1). The effects on the Ca^{2+} affinity when either one, two, or all of Glu17, Asp19, and Glu26 were substituted by the corresponding amides were considerable. The results, as well as the salt dependence of the observed effects, were in good agreement with electrostatic calculations (Svensson et al., 1990). Surprisingly, however, the substitution of Gln for Glu60 led to only a small decrease in the Ca^{2+} affinity. This effect seemed to be at variance with the electrostatic calculations. The discrepancy led to the suggestion that the side chain of Glu60 plays a direct structural role in the calcium-binding process, a role that could also be fulfilled by a Gln residue. In the high-resolution crystal structure of Ca^{2+}-loaded calbindin D_{9k} (1.6 Å; Svensson et al., 1992), one carboxylate oxygen of Glu60 is hydrogen bonded to the water molecule which provides its oxygen to calcium coordination in the N-terminal Ca^{2+} site (site I) (cf. Figure 2). Residue 60 thus plays a unique dual role by taking part in Ca^{2+} binding at both sites, since it provides its carbonyl oxygen to calcium coordination in the C-terminal site (site II). Another interesting feature is that Gln22 seems to fill a similar function. In this case, the carbonyl oxygen coordinates the calcium ion in site I (in the ligand position homologous to that of the Glu60 carbonyl oxygen in site II) while the oxygen of the side chain is hydrogen bonded to the water molecule which is a Ca^{2+} ligand in site II (cf. Figure 2).

We have now further analyzed the role of residue 60 in the calcium-binding process of calbindin D_{9k}. As a complement to the previously studied mutant (E60Q) with reduced negative charge and conserved size, we have now produced a mutant (E60D) with conserved negative charge but with reduced side chain length by substituting Asp for Glu60. The E60D mutant has been characterized by a range of experimental methods. Macroscopic calcium-binding constants have been measured using the chelator competition method, and the calcium-binding process has also been followed by ^1H NMR. The binding properties of the Ca^{2+} substitution probe Cd^{2+} have been studied using both ^{113}Cd and ^1H NMR. The stability toward thermal unfolding has been measured using differential scanning calorimetry. ^1H NMR chemical shift analysis shows that structural changes, if any, are confined to the loop regions. To quantify this observation, we have established the structural consequences of the Glu60→Asp substitution by X-ray crystallography.

MATERIALS AND METHODS

Chemicals. 5,5′-Br_2-BAPTA[1] was from Eugene, OR. Quin 2 was from Fluka, Switzerland. All other chemicals were of the highest purity commercially available.

Protein. The E60D mutant was expressed in *Escherichia coli* and purified as described in detail elsewhere (Johansson et al., 1990). The purity was checked by agarose gel electrophoresis in the presence of either 1 mM EDTA or 2 mM $CaCl_2$, isoelectric focusing, SDS–PAGE, and ^1H NMR.

Macroscopic Ca^{2+}-Binding Constants. The definitions of macroscopic (K_1 and K_2) and microscopic (K_I, K_{II}, $K_{I,II}$, and $K_{II,I}$) binding constants are outlined in Figure 3. The macroscopic Ca^{2+}-binding constants of E60D were determined from Ca^{2+} titrations in the presence of a chromophoric chelator in 2 mM Tris/HCl, pH 7.5. This method and data analysis are described in greater detail in a recent publication [see Linse et al. (1993)]. Separate titrations were first performed using either quin 2 or 5,5′-Br_2-BAPTA as chelator. Both chelators gave identical results, but the precision in the obtained binding constants was higher when 5,5′-Br_2-BAPTA was used. This chelator was therefore selected for triplicate titrations of solutions with high (0.15 M) and low (no added) KCl.

NMR Spectra. ^1H NMR spectra were recorded on a GE Omega 500 spectrometer operating at 500.13 MHz. One-dimensional spectra were recorded in D_2O at room temperature. Two-dimensional spectra—COSY, TOCSY (80 ms mixing time), and NOESY (200 ms mixing time)—were

[1] Abbreviations: Tris, tris(hydroxymethyl)aminomethane; 5,5′-Br_2-BAPTA, 5,5′-dibromo-1,2-bis(*o*-aminophenoxy)ethane-*N*,*N*,*N*′,*N*′-tetraacetic acid; quin 2, 2-[[2-[bis(carboxymethyl)amino]-5-methylphenoxy]-methyl]-6-methoxy-8-[bis(carboxymethyl)amino]quinoline; EDTA, ethylenediaminetetraacetic acid; SDS–PAGE, sodium dodecyl sulfate polyacrylamide gel electrophoresis; COSY, *J*-correlated spectroscopy; TOCSY, total correlation spectroscopy; NOESY, NOE spectroscopy; NOE, nuclear Overhauser enhancement.

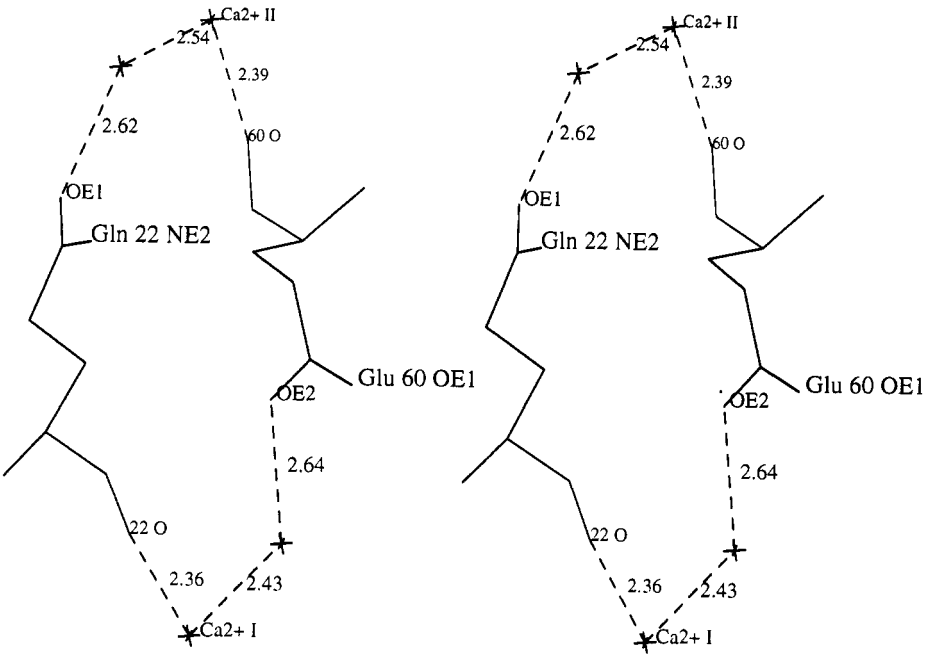

FIGURE 2: Stereographic plot of the symmetrical binding pattern of the two Ca^{2+} ions found in the crystallographic structure of native calbindin D_{9k} by Svensson et al. (1992). I and II denote Ca^{2+}-binding loops I and II; distances are marked in angstroms. The plot was produced by O and OPLOT (Jones et al., 1991).

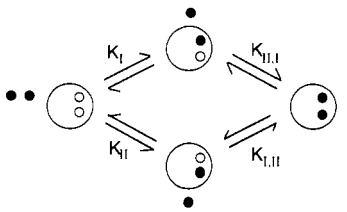

$$P + Ca^{2+} \overset{K_1}{\rightleftharpoons} P{\cdot}Ca \qquad P{\cdot}Ca + Ca^{2+} \overset{K_2}{\rightleftharpoons} P{\cdot}Ca_2$$

FIGURE 3: Definitions of macroscopic (K_1 and K_2) and microscopic (K_I, K_{II}, $K_{I,II}$, and $K_{II,I}$) calcium-binding constants. $K_1 = K_I + K_{II}$. $K_2 = K_{II} \cdot K_{I,II}/(K_I + K_{II})$.

recorded in H_2O, 27 °C, for 2 mM E60D either in the calcium free form at pH 5.25 or with slightly more than 2 equiv of calcium added at pH 6.0. The same set of spectra were also recorded for wild-type calbindin D_{9k} in the calcium free form at pH 5.25. ^{113}Cd NMR spectra were obtained on a home-built spectrometer using a solenoid probe and an Oxford Instruments 6T magnet at 56.55 MHz at room temperature and pH 6.5.

Differential Scanning Calorimetry (DSC). Each protein (E60D, E60Q, or the wild-type) was dissolved in 20 mM PIPES, 2 mM EDTA at pH 7.0. The protein concentration was 600 μM (5 mg/mL). All calorimetric scans were performed with a microcal MC-2 differential scanning calorimeter. The calorimetric unit was interfaced to a Victor PC computer using an A/D converter board (Data Translation DT-2801) for automatic data collection and analysis.

X-ray Crystallography. Lyophilized E60D protein was dissolved to a concentration of 35 mg/mL in 10 mM $CaCl_2$. Crystals were obtained with the hanging-drop method by mixing equal amounts of protein solution and 80% concentrated ammonium sulfate, which was also used as reservoir solution. The pH of the reservoir solution was titrated to 8.3 prior to the mixing. The obtained space group was $P2_1$ with the cell dimensions a = 29.1, b 41.4, and c = 55.2 Å and β = 96.5°. The asymmetric unit contained two independent molecules. The crystals grew to maximum dimensions of 0.25 × 0.1 × 0.05 mm^3 and diffracted to a maximum of 2.05 Å on a Rigaku RU200BEH rotating Cu anode running at 45 kV and 90 mA and with a focus of 0.3 × 3.0 mm. Diffraction patterns were collected with a Siemens X1000 area detector system and evaluated with the program XDS (Kabsch, 1988). The completeness of the data was 93% to 2.05 Å resolution, and the calculated R(SYM) value was 0.061.

The molecular replacement method, using the MERLOT program system (Fitzgerald, 1988), was used for the structure determination. The wild-type structure determined to 1.6 Å resolution (Svensson et al., 1992; code 4ICB in the Protein Data Bank) was used as a starting model. The positioned model was then subjected to crystallographic least squares refinement using the program X-plor (Brünger, 1989). The mutated amino acid residue 60 was originally refined as an alanine but at a later stage of the refinement, and after inspection of difference maps using the program O (Jones et al., 1991), it was introduced as an aspartate residue together with water molecules. The two molecules in the asymmetric unit were refined independently of each other. The final R value was 0.158 for data between 8.0 and 2.05 Å. Root-mean-square deviations from an ideal model were 0.014 Å for bond lengths, 2.9° for angles, and 23.2° for dihedral angles. Estimates of the overall errors in atomic positions of the structures, according to Luzzati (1952), are 0.20 Å for both the wild-type structure (Svensson et al., 1992) and the E60D structure. The low-temperature factors in the Ca^{2+} loops show that they constitute the most stable parts of the molecule. The true positional errors are hence probably less than 0.20 Å in those regions.

RESULTS

Expression and Purification. Expression levels in *E. coli* and yields after purification were as high as for many other calbindin D_{9k} mutants, or 40 mg of purified protein/L of culture medium. An agarose gel electrophoresis run in the presence of 1 mM EDTA for wild-type, E60Q, E60D, and two other mutant calbindin D_{9k}'s is shown in Figure 4. The

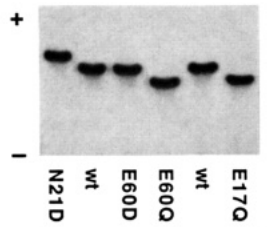

FIGURE 4: Agarose gel electrophoresis run in the presence of 1 mM EDTA. The protein run in each lane is indicated below the lane. wt = wild type.

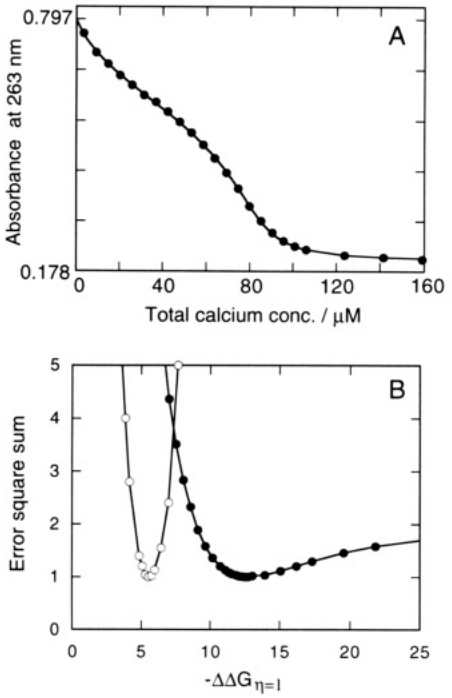

FIGURE 5: (A) One Ca^{2+} titration of 35 μM E60D in the presence of 30 μM 5,5′-Br_2-BAPTA and 0.15 M KCl, in 2 mM Tris/HCl buffer at pH 7.5. Absorbance at 263 nm versus total calcium concentration: (●) experimental points and (—) calculated curve with optimal fit to the data. This fit yielded log K_1 = 5.2 and log K_2 = 6.7 (B) (●) Error square sum of the fit to experimental points in panel A as a function of $-\Delta\Delta G_{\eta=1}$. Each point represents the lowest possible error square sum for a fixed value of $-\Delta\Delta G_{\eta=1}$, obtained by keeping the ratio of K_2 over K_1 fixed, while letting all other parameters including the individual values of K_1 and K_2 adjust their values to find the optimal fit. (○) Error square sum of the fit to one titration of wild-type calbindin D_{9k} as a function of $-\Delta\Delta G_{\eta=1}$.

relative mobilities of these zero or single mutants are governed by their respective total charge. The two mutants used as references are N21D (Asn21→Asp) with increased negative charge by 1 unit and E17Q (Glu17→Gln) with reduced negative charge by 1 unit. The agarose gel shows that E60D has the same mobility as the wild-type and E60Q has the same mobility as E17Q, as expected from their respective total charges.

Macroscopic Calcium-Binding Constants. One titration of E60D with Ca^{2+} in the presence of the chromophoric chelator 5,5′-Br_2BAPTA is shown in Figure 5A, and the results at high (0.15 M) and low (no added) KCl concentrations are listed in Table 1. At low ionic strength, the total affinity of binding two Ca^{2+} ions (i.e., the product of the two macroscopic binding constants, K_1K_2) in E60D has decreased by a factor of 38, in comparison with the wild-type protein. This corresponds to a 9.0 kJ mol^{-1} increase in ΔG_{tot}, the free energy of binding two Ca^{2+} ions ($\Delta G_{tot} = -RT \ln(K_1K_2)$). At high ionic strength (0.15 M KCl), we find that the Ca^{2+} affinity

Table 1: Ca^{2+}-Binding Parameters[a]

protein	[KCl] (M)	$\log_{10} K_1$	$\log_{10} K_2$	ΔG_{tot} (kJ mol^{-1})	$-\Delta\Delta G_{\eta=1}$ (kJ mol^{-1})
wt[b]	≤0.002	8.2	8.6	−96.2	6.9 ± 1.0
	0.15	6.3	6.5	−73.4	5.5 ± 0.6
E60D	≤0.002	≤6.9	≥8.4	−87.2	≥12
	0.15	≤5.4	≥6.5	−68.3	≥10
E60Q[b]	≤0.002	8.0	8.5	−94.4	6.1 ± 1.0
	0.15	6.6	6.2	−73.3	1.6 ± 0.5

[a] Macroscopic Ca^{2+}-binding constants, K_1 and K_2, free energy of binding two Ca^{2+} ions, $\Delta G_{tot} = -RT \ln(K_1K_2)$, and a lower limit to the free energy of interaction between the two sites, $-\Delta\Delta G_{\eta=1} = RT \ln(4K_2/K_1)$. [b] Data from Linse et al. (1991).

of E60D is a factor of 8 lower than in the wild-type. Almost all of the observed reduction in total affinity pertains to the first binding step. The low value observed for the first macroscopic binding constant K_1 implies that the affinities are reduced for both individual sites in the apo protein, i.e., both K_I and K_{II} are reduced (since both K_I and K_{II} are in the range (0.5–1.5) × 10^8 M^{-1} in the wild-type protein). The cooperativity of Ca^{2+} binding is significantly higher in E60D than in the wild-type, both at high and low ionic strength. Therefore the individual macroscopic binding constants are much less well determined than their product.

The cooperativity parameter that can be deduced from the titrations in the presence of a chelator is $-\Delta\Delta G_{\eta=1} = RT \ln(4K_2/K_1)$, which is a lower limit to $-\Delta\Delta G$, the free energy of interaction between the sites (Linse et al., 1991). Since this is a function of the *ratio* of the two macroscopic binding constants, it is inherently difficult to determine with high precision and uncertainties become larger the higher the value of $-\Delta\Delta G_{\eta=1}$. When $-\Delta\Delta G_{\eta=1}$ is close to 10 kJ mol^{-1} or above, the shape of the titration curve changes very little even with rather large changes in $-\Delta\Delta G_{\eta=1}$. This is clearly shown in Figure 5B, in which the error square sum of the optimal fit to experimental points is drawn as a function of $-\Delta\Delta G_{\eta=1}$, in comparison with the wild-type. Repeat experiments consistently show the same picture. We can thus conclude that the increase in $-\Delta\Delta G_{\eta=1}$ is significant. At low ionic strength, $-\Delta\Delta G_{\eta=1}$ has increased from 6.9 ± 1.0 kJ mol^{-1} in the wild-type protein to 12 kJ mol^{-1} or more in E60D. At 0.15 M KCl, the increase is from 5.5 ± 0.6 to 10 kJ mol^{-1} or more.

Ca^{2+} Binding as Monitored by ^1H NMR. One Ca^{2+} titration of E60D (in the absence of chelator) was followed by recording one-dimensional ^1H NMR spectra at each titration point. This titration shows the same general features as a corresponding titration of the wild-type calbindin D_{9k}. The first two Ca^{2+} ions bound are in slow exchange with free calcium ions, in good agreement with the observation of two high-affinity sites by the chelator method. The ^1H NMR titration has the capability of providing estimates of the relative affinities for the two sites in the protein, given that the macroscopic binding constants are known [see, for example, Linse et al. (1991)]. In the case of E60D, the cooperativity is so high that the only significantly populated species in the titration are the apo and Ca_2 forms. The total amount of the two Ca_1 forms, at the point where 1 equiv of calcium has been added, is as low as 2% of the total protein concentration. Therefore any estimate of relative affinities for the two sites will be highly uncertain. However, since $-\Delta\Delta G$ has been determined for the wild-type protein as 7.7 ± 1.7 kJ mol^{-1} at low salt and 4.6 ± 0.9 kJ mol^{-1} at 0.15 M KCl, we can conclude that in E60D the cooperativity is strongly enhanced and $-\Delta\Delta G$ has increased by ca. 5 kJ mol^{-1}.

Table 2: ^{113}Cd NMR Chemical Shifts for Cd^{2+} Ions Bound to Calbindin Wild-Type and Mutant and ^{113}Cd Shift Displacement, $\Delta\delta_{II,I}$, of the Site II Shift on Cd^{2+} Binding to Site I

	≤1 equiv of Cd	2 equiv of Cd		
protein	site II	site II	site I	$\Delta\delta_{II,I}$
wt[a]	−105	−110	−156	5
E60D	−102.3	−109.2	n.o.	7
E60Q[a]	−106.9	−111.8	n.o.	5

[a] Data from Linse et al. (1991); n.o. = not observed.

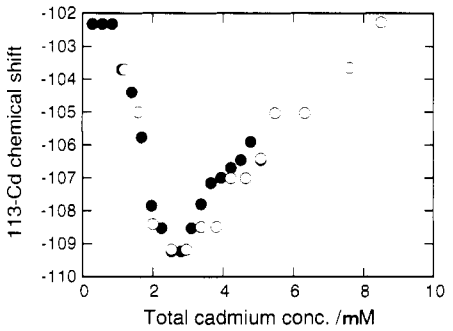

FIGURE 6: ^{113}Cd NMR chemical shift, δ, of the Cd^{2+} ion bound to site II of E60D as a function of total Cd^{2+} concentration. The protein concentration was ca. 0.85 mM. Two individual titrations are shown with open and filled symbols, respectively.

Cd^{2+} Binding as Monitored by ^{113}Cd NMR. A Cd^{2+} titration of E60D (using isotope enriched $^{113}Cd(NO_3)_2$) was followed by recording ^{113}Cd NMR spectra at each titration point. This titration shows the same general features as observed for the wild-type protein (Linse et al., 1987). Cadmium binds to the two Ca^{2+} sites in a sequential manner with site II filled first. At additions of $^{113}Cd^{2+}$ up to 1 equiv, a narrow signal appears at −102.3 ppm (cf. Table 2) and the intensity increases gradually. At additions of $^{113}Cd^{2+}$ between 1 and 2 equiv, the ^{113}Cd resonance is gradually shifted upfield to −109.2 ppm. The signal from ^{113}Cd in site I could not be observed at room temperature. Binding of the first Cd^{2+} ion to the C-terminal site is thus a slow exchange process, whereas Cd^{2+} binding to the N-terminal site is a fast exchange process. The displacement of the site II shift on Cd^{2+} binding to site I, $\Delta\delta_{II,I}$ has a value of −6.9 ppm in the present mutant (E60D) with increased cooperativity. This is somewhat larger than the value obtained for the wild-type protein [−5 ppm, Linse et al. (1987)]. It has previously been found that $\Delta\delta_{II,I}$ is lowered in mutants with decreased cooperativity (Linse et al., 1991). Hence there is a strong correlation between the value of the chemical shift displacement $\Delta\delta_{II,I}$ and the free energy of interaction between the binding sites.

On cadmium additions of between 2 and 6 equiv, the resonance of ^{113}Cd in site II gradually shifts back downfield, and at 6 equiv, it has reached −102 ppm. The experiment was stopped at that point although the additional binding process was not finished. The chemical shift as a function of added $^{113}Cd^{2+}$ is shown in Figure 6.

Cd^{2+} Binding as Monitored by ^1H NMR. A second Cd^{2+} titration of E60D (using unenriched $Cd(NO_3)_2$) was monitored by recording ^1H NMR spectra at each titration point. This titration confirms the results of the ^{113}Cd NMR studies, that the first 2 equiv of Cd^{2+} are bound sequentially, the first one in slow exchange and the second one in fast exchange. Additional Cd^{2+} ion(s) are bound with low affinity and are in fast exchange with free Cd^{2+} ions. The titration was continued up to 20 equiv of Cd^{2+}, where the third weak binding process was roughly 95% complete. The affinity of E60D for this third (or more) Cd^{2+} was found to be as low as 10^2–10^3 M^{-1} (as inferred from computer fits to the chemical shifts as a function of total calcium concentration).

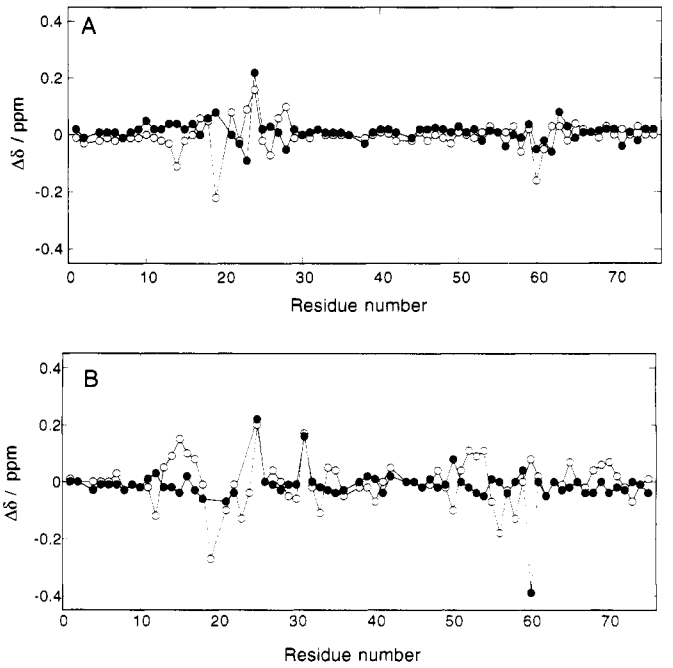

FIGURE 7: Differences in backbone ^1H NMR chemical shifts (mutant minus wild-type) for E60D (○) NH and (●) $C^{\alpha}H$. The data for residue 60 is corrected for the difference in random coil chemical shifts between Asp and Glu. (A) Calcium-loaded state. (B) Calcium free state.

Since this phenomenon of additional Cd^{2+} binding to calbindin D_{9k} has not been reported previously, we also made a titration of the wild-type protein with Cd^{2+}. This titration was continued up to 40 equiv of Cd^{2+} and followed by ^1H NMR. Also for the wild-type, we found that after the first two Cd^{2+} ions have been bound, additional Cd^{2+} ion(s) are bound. In this case, the process was roughly 95% complete at 40 equiv and the binding curve is not as steep as for E60D, indicating a lower affinity for the third (or more) Cd^{2+} ion.

Stability toward Thermal Unfolding. The stability toward thermal unfolding was measured using differential scanning calorimetry for the calcium free forms of E60D as well as E60Q. The thermal stabilities of these two mutants do not deviate much from that of the apo wild-type for which the transition midpoint of thermal denaturation (T_m) occurs at 85 ± 0.5 °C. For apo E60D, T_m has decreased to 84 ± 0.5 °C, and for apo E60Q, it has increased to 88.8 ± 0.5 °C.

^1H NMR Chemical Shift Analysis. The backbone ^1H NMR resonances were assigned for (the trans pro-43 form of) E60D in the apo as well as Ca_2 forms. Since the published apo shifts are for the P43G mutant (Skelton et al., 1989), we have also assigned the apo wild-type. The chemical shifts of the Ca_2 form of the wild-type were taken from Kördel et al. (1989). In both the apo and Ca_2 forms, the deviations from the published chemical shifts (Kördel et al., 1989; Skelton et al., 1989) were small enough that the majority of resonances could be assigned by comparison of the COSY and TOCSY spectra with those of the wild-type or P43G. The same was found for the wild-type relative to P43G. These tentative assignments were confirmed by the NOESY spectrum, which also helped to identify the remaining cross-peaks. The difference in NH and $C^{\alpha}H$ chemical shifts relative to the wild-type are shown in Figure 7. Note that in Figure 7 the data for residue 60 are corrected for the difference in random

coil chemical shifts between Glu and Asp residues. In the calcium-loaded state (Figure 7A), the chemical shift perturbations are below 0.25 ppm for all backbone resonances. All significant changes, except for at the mutated residue, are found in site I. The largest effects are observed for Asp19 $C^{\alpha}H$ (–0.23 ppm), Ser24 $C^{\alpha}H$ (0.21 ppm), Ser24 NH (0.17 ppm), and Asp60 NH (0.14 ppm). It is also noticeable that the largest effects on $C^{\beta}H$ chemical shift are observed for residues 19 and 22. One $C^{\beta}H$ resonance of residue 22 has shifted by 0.29 ppm. We have not made stereospecific assignments and can therefore only say that each $C^{\beta}H$ resonance of residue 19 has shifted by a minimum of 0.29 ppm and a maximum of 0.67 ppm (the $C^{\beta}H$ chemical shifts are 2.64 and 2.87 ppm in the wild-type but 2.20 and 2.35 ppm in E60D). In the apo state (Figure 7B), all chemical shift effects are below 0.25 ppm, except for residue 60. The $C^{\alpha}H$ chemical shift of residue 60 is 5.02 ppm in apo E60D and 4.94 ppm in the wild-type apo form. However, if we take the difference in random coil shift into account, there is an apparent effect of –0.39 ppm in E60D. The observed significant effects on backbone resonances involve more residues in the apo state than in the calcium state. Several of these residues are located in site II. For side chain proton, the largest effects are observed for residues 22 (–0.08 ppm for one $C^{\beta}H$) and 54 (–0.21 ppm for one $C^{\beta}H$).

X-ray Crystallography. A comparison between the crystallographic results for the Ca^{2+}-loaded states of the wild-type calbindin D_{9k} (Svensson et al., 1992) and the E60D mutant shows small differences. The largest difference found is the different packing arrangements of the molecules in the crystals. The wild-type packs by one molecule in the asymmetric unit, whereas for E60D the asymmetric unit contains two molecules with slightly different structure. The two independent molecules of E60D, which will be referred to as molecules A and B, are oriented in such a way that a close contact is formed between two calcium loops. The distance from the Ca^{2+} ion in loop I in molecule A is about 11 Å to the Ca^{2+} ion in loop II of molecule B (Figure 8). This is about the same number as for the intramolecular loop I–loop II Ca^{2+}–Ca^{2+} distance.

Packing of the E60D molecules is achieved by replacing two water molecules found in the wild-type structure with two of the main chain carbonyl oxygens from loop II of molecule B. One of these water molecules is well defined in the wild-type structure (its B value is 22 Å^2), and it is hydrogen bonded to the Ca^{2+}-coordinating water in loop I. In the E60D crystal, there is no corresponding water molecule and a strong hydrogen bond is instead formed between the Gly57 carbonyl oxygen of molecule B and the calcium-coordinating water in molecule A (distance 2.62 Å). The second replaced water molecule is less well defined in the wild-type structure (B = 34 Å^2), and it is hydrogen bonded to another water molecule which in turn is hydrogen bonded to the Lys25 backbone amide nitrogen of molecule A. In the E60D crystal, it is replaced by the Asn56 carbonyl oxygen of molecule B. In the E60D crystal, the distances Asn56 carbonyl–water–Lys25 amide nitrogen are considerably longer than the distances Gly57 carbonyl–water–Ca^{2+}, indicating that the major forces between the A and B molecules exist at the Gly57 connection.

The difference in intermolecular connections for the two independent E60D molecules in the asymmetric unit causes molecules A and B to have slightly different conformations. The results of least squares superposition of the C_{α} atoms of the wild-type structure and the C_{α} atoms of the E60D mutant molecules A or B, respectively, are shown in Table 3. These data show that molecule B resembles the wild-type structure more than does molecule A. The difference is most prominent (but still small) in the region of calcium site I as shown in the stereographic overlays of the wild-type with either molecule A or B (Figure 9). In both molecules A and B, the Asp60 residue tries to accommodate to the conformation of Glu60 in the wild-type structure. Clearly, this cannot be done precisely, due to the shorter side chain of aspartate. Therefore the hydrogen bond between the Asp60 carboxylate group and the Ca^{2+}-coordinating water has become longer than for the wild-type Glu60. This is true for both molecules A and B. Distances for wild-type and molecules A and B were found to be 2.64, 2.93, and 2.82 Å, respectively. The other carboxylate oxygen of residue 60 is hydrogen bonding a second water molecule, both in the wild-type structure and in molecule B, while for molecule A this is not possible due to the tight crystal packing to molecule B.

The largest differences, except at the mutated residue 60, are observed in molecule A at Gly18, the main chain and side

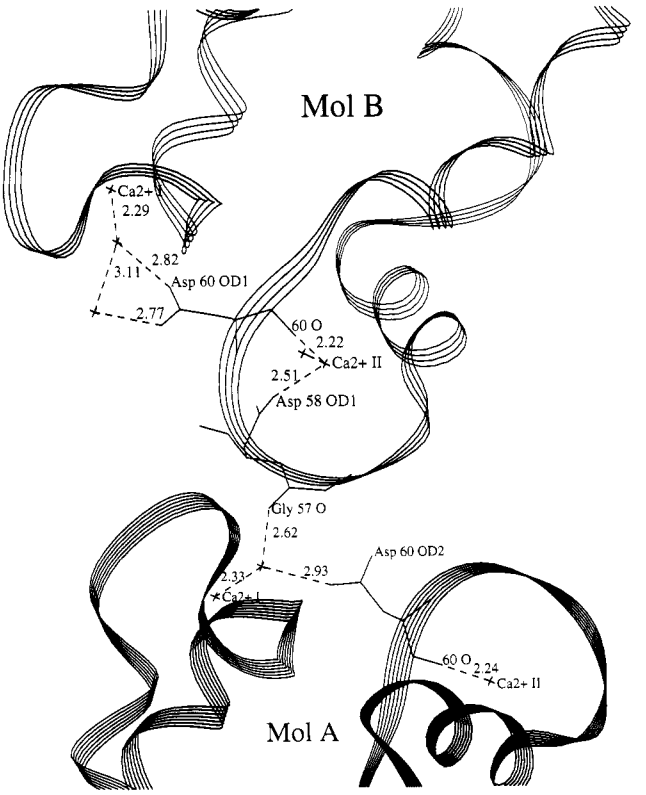

FIGURE 8: Crystal packing of the two crystallographically independent molecules of E60D-mutated calbindin D_{9k}. The molecules are denoted A and B. The C_{α} stretch of molecule A is plotted as a 7-stranded ribbon diagram and that of the B molecules as a 4-stranded diagram. Distances between atoms are in angstroms. I and II denote Ca^{2+}-binding loops I and II in calbindin counted from the N-terminal. The plot was produced by O and OPLOT (Jones et al., 1991).

Table 3: Crystallographic rms Values[b]

	rms deviations (Å)	
	all	Ca^{2+} loops
wt–mol A	0.86	0.36
wt–mol B	0.34	0.22
mol A–mol B	0.84	0.47

[a] Root-mean-square (rms) deviations in angstroms between the wild-type (wt) structure of calbindin D_{9k} and the two crystallographically independent molecules A and B of the E60D mutant. rms values are given for least squares superpositioning of all C_{α} atoms, columns "all", and for superpositioning of C_{α} atoms for residues 14–27 and 54–65 (the two Ca^{2+}-binding loops), column "Ca^{2+} loops". Superpositionings were made using the program O (Jones et al., 1991).

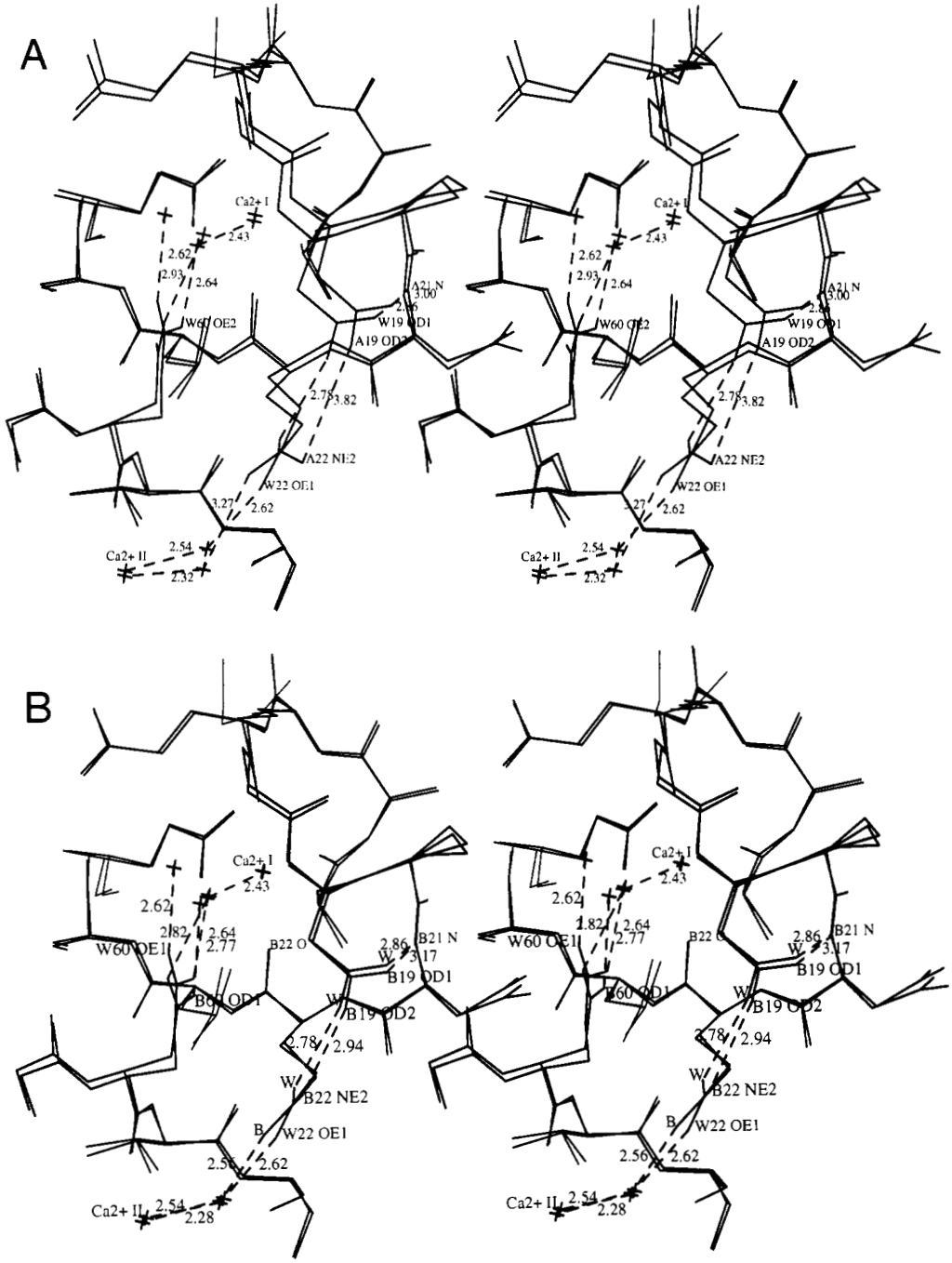

FIGURE 9: Comparison of the crystal structures of E60D and wild-type in their calcium-loaded states. A stereoplot of calbindin Ca^{2+}-binding loop I and parts of loop II. (A) Molecule A of E60D-mutated calbindin is superimposed on the wild-type structure. (B) Molecule B is superimposed. The wild-type structure is denoted W, while the A and B molecules of E60D are denoted A and B. Distances for some bonds are given in angstroms. The plot was produced by O and OPLOT (Jones et al., 1991).

chain of Asp19, and the side chain of Gln22 (cf. Figure 9A). The hydrogen bond found in the wild-type structure between one of the carboxylate oxygens of Asp19 and the side chain amide nitrogen of Gln22 (distance 2.78 Å) is lost in molecule A of E60D (distance 3.82 Å). The side chain amide group of Gln22 is rotated 42° as compared to the wild-type configurations, and the distance between its oxygen atom and the Ca^{2+}-coordinating water in loop II has increased from 2.62 to 3.27 Å. Instead, the distance from the coordinating water to Ca^{2+} has decreased from 2.54 to 2.32 Å.

The differences between molecule B and the wild-type structure are smaller than for molecule A. Most differences are probably within the error limits, except for the water to Ca^{2+} distance in site II. This distance has a value of 2.28 Å in the B molecule, almost the same as in the A molecule, but significantly shorter than the value observed in the wild-type (2.54 Å, cf. Figure 9).

For both molecules A and B, we find that the differences from wild-type calbindin D_{9k} are much less pronounced within loop II than in loop I. The very small differences observed for Ca^{2+}-binding loop II are all within the error limits, except for the water–Ca^{2+} distance as mentioned above.

DISCUSSION

The seemingly modest charge-conserving alteration Glu60→Asp in the calbindin D_{9k} mutant E60D has been found to reduce the total Ca^{2+} affinity and increase the cooperativity of Ca^{2+} binding. At first glance, these results appear a bit surprising as were the effects of the alteration Glu60→Gln

in the mutant E60Q, which resulted in reduced cooperativity and a very small reduction in total affinity (Linse et al., 1991). The side chain of the Glu60 residue is located in close proximity to both calcium ions. If the side chain of Glu60 was merely a surface charge, one would expect a considerable electrostatic contribution to the calcium affinity at both sites. In such a case, E60Q with reduced negative charge, but not E60D with conserved charge, would be expected to have a drastically reduced calcium affinity at both sites. This is, however, not observed, and therefore the Glu60 side chain is likely to have a more direct structural involvement in the calcium-binding process. It is possible to arrive at an explanation for the observed mutational effects at position 60 if we assume that also in solution the Glu60 carboxylate is hydrogen bonded to the water molecule which is a calcium ligand in site I. The hydrogen bond is likely to stabilize the calcium-coordinating water molecule, thereby making it a better calcium ligand. The side chain of Gln has a similar length as that of Glu and might form an equally strong hydrogen bond to the calcium-coordinating water. This could be part of the reason for the calcium affinity of E60Q being almost as high as in the wild-type. When, on the other hand, the side chain is shortened by one methylene unit, as in E60D, it is reasonable to expect a weaker hydrogen bond to the water ligand. This could make the water molecule a less favorable calcium ligand, leading to reduced affinity. Alternatively, we might speculate about perturbations of the binding site in its calcium free state as the primary cause of the reduced affinity. If a water molecule is captured already in this state by a hydrogen bond to the carboxylate in position 60, the incoming Ca^{2+} ion can release all water molecules in the hydration shell, giving rise to a large favorable entropic contribution to the affinity. If in such a case shortening of the side chain of residue 60 leads to a weaker carboxylate–water interaction, release of the hydration water of the incoming Ca^{2+} ion might not be as complete and the favorable entropic contribution to the affinity might be reduced in comparison with the wild-type protein.

Of considerable interest here is the crystallographic structure determination for E60D, the main result of which is that the structure of the mutant is nearly identical to that of the wild-type. The similarity in the structures is mirrored by the very small differences in the T_m values as determined by DSC. The regions of the protein where small but significant perturbations are observed include, besides residue 60, primarily residues Gln22 and Asp19. This result is paralleled by the observation from ^1H NMR chemical shift analysis that Gln22 and Asp19 are the two residues in E60D for which the largest $C^\beta H$ chemical shift perturbations are observed in the Ca_2 form. In addition, all significant backbone chemical shift perturbations observed occur in the same area as where crystal structure changes are observed. In this context, it is also worth considering that several calbindin D_{9k} mutants for which altered cooperativity has been observed have substitutions in this particular region. These mutants are E17Q and D19N (Linse et al., 1991), E60Q (Linse et al., 1991), and E60D (this study). If we focus on the Asp60 residue, we see that its side chain stretches toward the water in site I as much as possible with minor disruption of the fold of site II, where the main chain carbonyl oxygen provides a calcium ligand (cf. Figure 9). The water to carbonyl oxygen distance in site I has increased slightly in E60D. A similar effect is observed for residue 22, for which there is an increase in the distance between the side chain oxygen and the calcium-coordinating water in site II. On the basis of the crystal structure, we can thus suggest that for both sites the reduced Ca^{2+} affinity is a consequence of less favorable water ligands.

The observed effects on cooperativity are difficult to rationalize in structural terms, and several ion ligation states must be considered. The crystallographic structure as presented here is determined for the mutant protein after it has bound two Ca^{2+} ions. It shows that the much higher cooperativity in E60D as compared to the wild-type is not caused by any extensive structural effects of the mutation on the Ca_2 state. The ^1H NMR chemical shift analysis indicates that the structural changes are very small also in solution. The data for the apo state indicates that the structural consequences of the E60D mutation are small also in this form but the chemical shift changes involve a larger region of the molecule than in the calcium form. This region extends also to site II. This finding connects to the calcium-binding constant determinations, which show that the largest reduction in calcium affinity pertains to the first binding step. For the P34G mutant of calbindin D_{9k}, ^1H NMR-derived solution structures are now available for the states with zero and two calcium ions bound (Kördel et al., 1993; Skelton et al., 1994). A comparison of these structures have shown that the overall response to calcium binding is much attenuated relative to the current models pertinent to calmodulin and troponin C (Skelton et al., 1994). Some of the side chains in the loop region are medium to well resolved also in the apo state. For example, the Glu60 and Gln22 side chains are found to point toward the opposite site also in this state (W. Chazin, personal communication). More substantial changes are seen in the flexibility in the loop region, which is observed to be reduced on binding of metal ions (Skelton, 1992; Akke, 1993). At the time of the writing, attempts to crystallize calbindin D_{9k} with less than 2 equiv of calcium have not been successful. It therefore remains to be specified to what extent the charged loop residues in positions 17, 19, and 60, which in mutagenesis studies have proben important for the cooperativity, undergo any substantial rearrangements or changes in mobility due to metal ion binding. It is, however, not likely that, in the absence of calcium, all charged residues retain the conformation of the calcium-loaded state, due to electrostatic repulsion. Available data on troponin C indicate a small expansion of the binding sites in the absence of Ca^{2+} (Saturshyr et al., 1988).

It is also important to ask whether the observed crystallographic differences between wild-type and E60D reflect structural effects of the mutation only or if the differences in crystal packing also contribute. Of considerable interest in this context is the fact that the E60D crystal contains two protein molecules in the asymmetric unit, with molecule B being more similar to the wild-type than is molecule A (cf. Figures 8 and 9). We believe that most of the perturbations found in molecule A of the E60D mutant (relative to molecule B) arise from the tight crystal packing between the molecules. It should be mentioned that crystal structures have been determined for two other mutant calbindins D_{9k} (D19N, and E17Q + D19N; unpublished results), both having altered cooperativity of Ca^{2+} binding. Both these mutants crystallize in the same type of crystal lattice as E60D. It is therefore relevant to ask if the mutation is causing the new packing, and if so, what do the differences between each pair among the wild-type, E60D molecule A, and E60D molecule B tell us. One could of course say that the A and B molecules represent two conformations with similar free energy that can be packed against each other in a favorable way.

CONCLUSIONS

Shortening of a charged side chain in calbindin D_{9k} (Glu60→Asp) leads to a markedly increased cooperativity of calcium binding. The total affinity of binding two calcium ions is, however, reduced. The crystal structural changes observed relative to the wild-type in the calcium-loaded crystalline state are very small and confined to the region around residues Asp19, Gln22, and Asp60. In solution, all structural changes due to the mutation occur in the same area as seen in the crystal state. A correlation is found between the cooperativity of calcium binding and the ^{113}Cd NMR chemical shift displacement of a $^{113}Cd^{2+}$ ion in site II as a consequence of cadmium entering site I.

REFERENCES

Akke, M., Forsén, S., & Chazin, W. J. (1991) *J. Mol. Biol. 220*, 173–189.

Akke, M., Skelton, N. J., Kördel, J., Palmer, A. G., III, & Chazin, W. J. (1993) *Biochemistry 32*, 9832–9844.

Brünger, A. T., Karplus, M., & Petsko, G. A. (1989) *Acta Crystallogr. A 45*, 50–61.

Carlström, G., & Chazin, W. J. (1993) *J. Mol. Biol. 231*, 415–430.

Finn, B. E., Kördel, J., Thulin, E., Sellers, P., & Forsén, S. (1992) *FEBS Lett. 298*, 211–214.

Fitzgerald, P. M. (1988) *J. Appl. Crystallogr. 21*, 273–278.

George, S. E., Su, Z., Fan, D., & Means, A. R. (1993) *J. Biol. Chem. 268*, 25213–25220.

Johansson, C., Brodin, P., Grundström, T., Forsén, S., & Drakenberg, T. (1990) *Eur. J. Biochem. 187*, 455–460.

Jones, T. A., Zou, J.-Y., Cowan, S. W., & Kjeldgaard, M. (1991) *Acta Crystallogr. A 47*, 110–119.

Kabsch, W. (1988) *J. Appl. Crystallogr. 21*, 916–924.

Kay, L. E., Forman-Kay, J. D., McCubbin, W. D., & Kay, C. M. (1991) *Biochemistry 30*, 4323–4333.

Kesvatera, T., Jönsson, B., Thulin, E., & Linse, S. (1994) *Biochemistry* (in press).

Kördel, J., Forsén, S., & Chazin, W. J. (1989) *Biochemistry 28*, 7065–7074.

Kördel, J., Skelton, N. J., Akke, M., & Chazin, W. J. (1993) *J. Mol. Biol. 231*, 711–734.

Linse, S. & Forsén, S. (1995) *Advances in Phosphoprotein Research 30*, 89–151.

Linse, S., Brodin, P., Drakenberg, T., Thulin, E., Sellers, S., Elmdén, K., Grundström, T., & Forsén, S. (1987) *Biochemistry 26*, 6723–6735.

Linse, S., Johansson, C., Brodin, P., Grundström, T., Thulin, E., & Forsén, S. (1988) *Nature 335*, 651–652.

Linse, S., Johansson, C., Brodin, P., Grundström, T., Darkenberg, T. & Forsén, S. (1991) *Biochemistry 30*, 154–162.

Linse, S., Thulin, E., & Sellers, P. (1993) *Protein Sci. 2*, 985–1000.

Luzzati, P. V. (1952) *Acta Crystallogr. 5*, 802–810.

Maune, J. F., Klee, C. B., & Beckingham, K. (1992) *J. Biol. Chem. 267*, 5286–5295.

McPhalen, C. A., Strynadka, N. C. J., & James, M. N. G. (1991) *Adv. Protein Chem. 42*, 77–144.

Reid, R. E. (1990) *J. Biol. Chem. 265*, 5971–5976.

Shaw, G. S., Golden, L. F., Hodges, R. S., & Sykes, B. D. (1991) *J. Am. Chem. Soc. 113*, 5557–5563.

Skelton, N. J., Forsén, S., & Chazin, W. J. (1990) *Biochemistry 29*, 5752–5761.

Skelton, N. J., Kördel, J., Akke, M., Forsén, S., & Chazin, W. J. (1994) *Nat. Struct. Biol. 1*, 239–245.

Svensson, B., Jönsson, B., & Woodward, C. (1990) *Biophys. Chem. 38*, 179–183.

Svensson, L. A., Thulin, E., & Forsén, S. (1992) *J. Mol. Biol. 223*, 601–606.

Szebenyi, D. M. E., & Moffat, K. (1986) *J. Biol. Chem. 261*, 8761–8777.

Trigo-Gonzalez, G., Awang, G., Racher, K., Neden, K., & Borgford, T. (1993) *Biochemistry 32*, 9826–9831.

Tsuji, T., & Kaiser, E. T. (1991) *Proteins: Struct. Funct. Genet. 9*, 12–22.

Waltersson, Y., Linse, S., Brodin, P., & Grunström, T. (1993) *Biochemistry 32*, 7866–7871.